

Effect of kinetic and electronic energy on the reactions of Mn^+ with H_2 , HD, and D_2

J. L. Elkind and P. B. Armentrout^{a)}

Department of Chemistry, University of California, Berkeley, California 94720

(Received 10 December 1985; accepted 29 January 1986)

Reactions of several electronic states of Mn^+ with H_2 , HD, and D_2 have been examined using guided ion beam mass spectroscopy. The excitation function for the ground state of Mn^+ (7S) has two regions: one of very low reactivity at threshold and another more efficient pathway at higher energies. In contrast, the 5S and 5D states react efficiently at their thermodynamic thresholds. In reaction with HD, the 5S and 5D states produce ≈ 3 times as much MnH^+ as MnD^+ in the threshold region. This isotope effect is similar to that seen in previous studies of transition metal ion reactions. Reaction of Mn^+ (7S) with HD, on the other hand, exhibits an extreme isotope effect such that MnD^+ is formed almost exclusively. The state dependence of the reactivity and reaction mechanisms is explained using simple molecular orbital concepts. The results are analyzed to yield a bond dissociation energy at 0 K for MnH^+ of 2.06 ± 0.15 eV (47.5 ± 3.4 kcal/mol).

INTRODUCTION

The reactions of atomic transition metal ions with a variety of small molecules are the subjects of intense current research. While most metal ions react readily, Mn^+ and Cr^+ show much lower reactivity.¹ The fact that both ions have very stable high spin half-filled $3d$ shells helps explain their relative inertness. In this paper we seek to explore further the anomalous reactivity of Mn^+ by a detailed examination of its simplest reaction, that with molecular hydrogen and its isotopic variants. Since the electronic configuration of Mn^+ is invoked to explain its reactivity, we are particularly interested in studying the influence of electronic excitation on these reactions.

The reaction of Mn^+ with H_2 :



has been studied once before although no details were published. From this ion beam study,^{1(a)} Armentrout, Halle, and Beauchamp reported a value for the MnH^+ bond energy of 53 ± 3 kcal/mol although unspecified difficulties in interpretation were encountered. However, this value agrees nicely with one determined by a gas-phase proton affinity measurement, 53 ± 5 kcal/mol.² Recent *ab initio* calculations provide much lower values, 40.8,³ 37.4,⁴ and 39.6⁵ kcal/mol. These authors⁵ suggest that discrepancies like this may be the result of not completely accounting for electronic excitation in the experiments. For this reason, the dependence of reaction (1) on the electronic state of the Mn^+ is expected to be particularly edifying.

Also of interest is a comparison with a similar study⁶ of the reactions of vanadium ions with H_2 , HD, and D_2 as a function of the electron configuration of V^+ . It was determined that while the ground and excited states of V^+ exhibit similar reactivity and yield the same thermochemistry, they appear to have very different reaction dynamics. These observations were rationalized using simple molecular orbital

concepts. One question the present study seeks to address is whether these simple molecular orbital ideas can be used to gain a *general* understanding of transition metal-hydrogen interactions.

EXPERIMENTAL

The ion beam apparatus used in these experiments has been described previously.⁷ The production of manganese ions is detailed below. The ions are extracted from the source, accelerated, and focused into a 60° magnetic sector for mass analysis. For these experiments the ^{55}Mn isotope (100% natural abundance) was used. The mass selected ion beam is decelerated to a selected kinetic energy and focused into an octopole ion trap which is floated at the nominal ion energy. The octopole guides the ions through the collision chamber containing the reactant gas. The pressure of the gas in the gas cell, measured by an MKS Baratron capacitance manometer, is in the range of 0.2–1.0 mTorr. This is sufficiently low that reactions due to multiple ion-molecule collisions are improbable. The octopole ion guide utilizes rf electric fields to trap ions in the radial direction and thus allows efficient collection of all ionic products and transmitted reactant ions. These ions are extracted from the octopole, focused into a quadrupole mass filter for mass analysis, and detected using a scintillation ion counter and standard ion counting techniques. A DEC MINC computer system controls the reaction conditions and data collection.

Ions are produced in two different sources. In the surface ionization (SI) source, a resistively heated oven is used to vaporize MnCl_2 . The vapor is directed at a rhenium filament which has been resistively heated to 2200 ± 100 K, as measured using optical pyrometry. The metal halide decomposes on this filament and metal ions are produced by surface ionization of the resulting metal atoms. If we presume that the metal reaches equilibrium at the filament temperature before desorption, the state distribution of the Mn^+ beam produced by SI should have a Maxwell-Boltzmann distribution. Previous studies⁸ in our lab on other metals

^{a)} NSF Presidential Young Investigator 1984–1989.

TABLE I. Electronic states of Mn⁺ below 3.5 eV.

State	Configuration	<i>E</i> (eV) ^a	Population (%) ^b
⁷ S	4s3d ⁵	0.0	99.83 ± 0.06
⁵ S	4s3d ⁵	1.175	0.145 ± 0.045
⁵ D	3d ⁶	1.808	0.026 ± 0.013
⁵ G	4s3d ⁵	3.419	<0.001

^aStatistical average over all *J* levels. Energies taken from C. Corliss and J. Sugar, *J. Phys. Chem. Ref. Data* 6, 1253 (1977).

^bMaxwell-Boltzmann distribution at 2200 ± 100 K.

indicate that this is a reasonable approximation. Table I lists the values calculated. It should be noted that if equilibrium is not reached, we would expect less excitation than Table I indicates.

In order to produce electronically excited metal ions, Mn₂(CO)₁₀ is introduced into an electron impact (EI) ionization source. Mn⁺ is formed when the electron energy (*E_e*) exceeds the appearance potential of Mn⁺ from Mn₂(CO)₁₀ (20.4 ± 0.4 eV).⁹ As the electron energy is increased, the probability of producing electronically excited ions increases. All of the low lying states of Mn⁺ are 4s3d⁵ or 3d⁶ configurations and therefore all transitions between these states are parity forbidden. For this reason we assume that the radiative lifetimes of the excited states exceed the 10–100 μs flight time of the ions between the source and the interaction region.¹⁰

Retarding field energy analysis is used to determine the nominal energy zero and distribution of the ion beam energy. This analysis is achieved by sweeping the dc bias of the octopole trap through the nominal ion energy zero. Because the reaction zone and this energy analysis region are physically the same, ambiguities in the analysis resulting from contact potentials, space charge effects, and focusing aberrations are avoided. From the derivative of the retarding curve, the true ion beam energy zero can be measured within 0.1 eV lab. In the center-of-mass frame, this introduces an energy uncertainty of <3.5, 5.2, and 6.8 meV for the H₂, HD, and D₂ systems, respectively. The ion beam energy distribution is found to have a typical FWHM of 0.7 eV lab (<25, 36, and 47 meV cm for the H₂, HD, and D₂ reactions, respectively). The effect of the thermal motion of the gas in the reaction cell contributes a much larger uncertainty to the collision energy. The resultant energy distribution effectively broadens any sharp features in the excitation function. Both this effect and the ion beam energy distribution are taken into account when analyzing the experimental results.¹¹

Reaction cross sections, σ , are calculated using

$$I_r = (I_r + I_p) \exp(-n\sigma l) \quad (2)$$

which relates the effective length of the interaction region, *l* (= 8.6 cm), and the number density of the target gas, *n*, to the measured intensities of the transmitted reactant ions and product ions, *I_r* and *I_p*. In the case of HD reactions, individual product cross sections are calculated using

$$\sigma(\text{MnH}^+) = \sigma I(\text{MnH}^+) / [I(\text{MnH}^+) + I(\text{MnD}^+)] \quad (3)$$

and similarly, $\sigma(\text{MnD}^+)$. The largest contribution to the uncertainty of our measurement of absolute cross sections results from uncertainties in the target gas density and effective cell length. We estimate these errors to be ± 20%. Absolute cross sections are measured by ensuring that *I_p* varies linearly with *n* at low pressures (thin target limit). In these experiments the quadrupole mass filter does not completely resolve the weak MH⁺ product signal from the intense M⁺ reactant. To correct for this, as well as for random counting noise, data is accumulated with reactant gas directed into the gas cell and directly into the vacuum chamber on alternate mass and energy sweeps. Subtraction of these data yields a signal due entirely to product ions formed in the cell.

Mn₂(CO)₁₀ is obtained from Alfa and is used without further purification except for multiple freeze-pump-thaw cycles. MnCl₂·4H₂O is obtained from Mallinckrodt and is used as is. HD has been prepared by standard procedures. Purity of > 95% HD was confirmed by mass spectrometric analysis. Impurities are primarily H₂ and D₂ in equal amounts.

RESULTS

Mn⁺(SI) + H₂, D₂

Figure 1 shows the experimental excitation function for the reaction of D₂ with a beam of manganese ions produced by surface ionization, SI. There are two easily discernable features. The dominant high energy feature reaches a maximum of 0.1 Å² at approximately 8.5 eV. Its threshold is obscured by the second, low energy feature but appears to be between 4 and 5 eV. This low energy feature has a threshold near 1.0 eV and reaches a plateau of ≈ 0.008 Å² between 3 and 4 eV. Data for the reaction of Mn⁺ with H₂ shows a

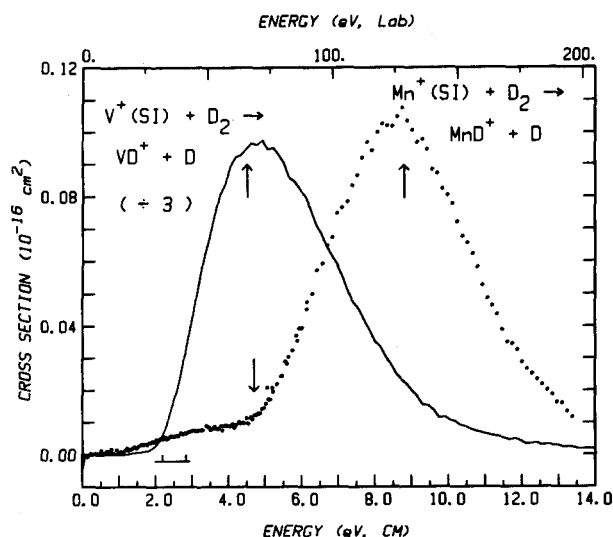


FIG. 1. Cross sections for reactions of Mn⁺ (points) and V⁺ (line) with D₂ as a function of kinetic energy in the center-of-mass frame (lower scale for both systems) and laboratory frame (upper scale for Mn⁺ system). Both ions are produced by surface ionization (SI). The results of V⁺ have been reduced by a factor of 3. The bracket shows the range of threshold energies expected for the Mn⁺(⁷S) reaction, see the text. Arrows indicate the threshold for product dissociation, process (4), at 4.5 eV, the pairwise threshold energy at 4.7 eV, and the pairwise dissociation energy at 8.8 eV, see the text and Table IV.

similar excitation function within experimental uncertainties.

This behavior is curious in several respects. More typical excitation functions^{6,12} for atomic metal ion- H_2 (or D_2) reactions have thresholds corresponding to the thermodynamic limit and reach maxima of $0.3\text{--}1.8 \text{ \AA}^2$ at an energy close to 4.5 eV. Above this energy, the MH^+ (MD^+) product can be formed with internal energies in excess of its dissociation energy. This corresponds to the onset of process (4),



which has a threshold equal to the bond energy of H_2 (D_2), 4.5 eV.¹³ An example of this typical behavior is shown for comparison in Fig. 1 by the results for $V^+(SI) + D_2$.⁶ The cross sections measured here for Mn^+ are not only smaller than usual but the peak position is shifted to high energies and the thresholds seem inconsistent with literature thermochemistry. The expected thermodynamic threshold, E_T , is given approximately by Eq. (5),

$$E_T = D^\circ(H_2) - D^\circ(MnH^+). \quad (5)$$

Using the experimental value^{1,2} for $D^\circ(MnH^+)$ of 53 ± 5 kcal/mol (2.3 ± 0.2 eV) yields $E_T = 2.2 \pm 0.2$ eV while the theoretical bond energies of 37.4 to 40.8 kcal/mol (1.62 to 1.77 eV)³⁻⁵ predict $E_T \approx 2.8 \pm 0.1$ eV. Clearly neither of these predictions is borne out by the data. Rather, the major feature appears to have a higher onset while the minor, low energy feature has a substantially lower threshold. Since it is unlikely that the literature thermochemistry is inaccurate by over 1 eV, these observations imply that the low energy feature is due to excited states of Mn^+ .

This conclusion is surprising since the reactant beam produced by surface ionization is expected to be very pure ground state Mn^+ , Table I. However, the SI source should also produce very small amounts of $Mn^+(^5S)$ and $Mn^+(^5D)$, Table I. If we assume that both these states can also react to form ground state MnH^+ , the thermodynamic threshold of the 5S state is 1.17 eV lower than that of the 7S state such that $E_T(^5S) = 1.0 \pm 0.2$ to $\approx 1.6 \pm 0.1$ eV, while the 5D state is 1.81 eV lower, $E_T(^5D) = 0.4 \pm 0.2$ to $\approx 1.0 \pm 0.1$ eV. Also, the maximum cross section expected should be reduced by the relative populations of these states. The low energy feature is quite consistent with these expectations. This leads us to conclude that the major high energy feature is due to reaction of $Mn^+(^7S)$ which apparently does not react efficiently until energies well in excess of the endothermicity. The low feature appears to be due to either $Mn^+(^5S)$, $Mn^+(^5D)$, or both.

$Mn^+(EI) + D_2$

These conclusions can be independently checked by examining the reactions of Mn^+ produced by electron impact (EI) ionization. Now, the ionization process is much more energetic and can lead to production of substantial amounts of excited Mn^+ . Figure 2 shows the results for Mn^+ produced by electron impact of $Mn_2(CO)_{10}$ at three electron energies, $E_e = 25, 30,$ and 50 eV. All three of these energies are well above the appearance potential of Mn^+ , 20.4 ± 0.4 eV.⁹ There is a clear trend that occurs with increasing E_e

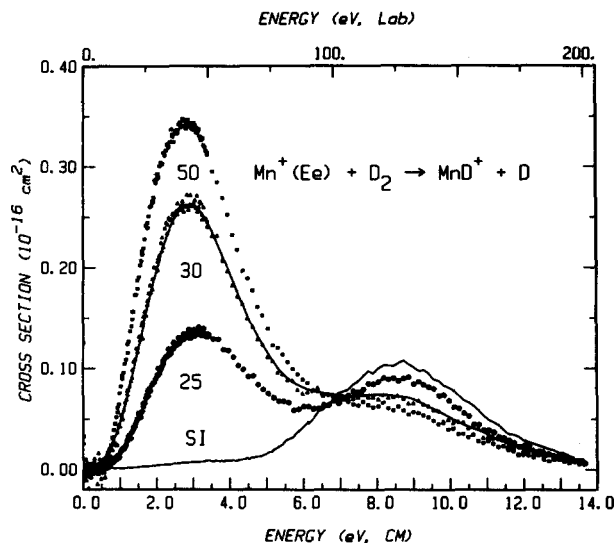


FIG. 2. Cross section for reaction of Mn^+ with D_2 as a function of kinetic energy in the center-of-mass frame (lower scale) and laboratory frame (upper scale). Data is shown for Mn^+ produced by electron impact at electron energies (E_e) of 50 eV (squares), 30 eV (triangles and line), and 25 eV (circles) and by surface ionization (SI, line). The latter data is the same as shown in Fig. 1.

which corresponds to an enhancement of the low energy feature and a depletion of the high energy one. Also, the apparent threshold is now about 0.6 eV and insensitive to electron energy. This behavior is completely consistent with the identification of the high energy feature as reaction due to the ground state of Mn^+ and the low energy feature as reaction due to excited states. The apparent threshold in the low energy feature is consistent with the thermodynamic threshold of either the 5S or 5D states of Mn^+ . The now prominent peak in the low energy feature at about 3 eV is also consistent with the 5S and 5D states. If all the electronic excitation, E_{el} , is available to reaction (4), the peak is expected at $D^\circ(H_2) - E_{el}$ which is 3.3 and 2.7 eV for the 5S and 5D states, respectively. The shift in apparent threshold from ≈ 1.0 eV for $Mn^+(SI)$ to ≈ 0.6 eV for $Mn^+(EI)$ may imply that the production of $Mn^+(^5D)$ increases relative to that of $Mn^+(^5S)$. Apparently, higher lying excited states of Mn^+ , Table I, are not appreciably populated since reactions of these states are exothermic and no features corresponding to such reactions are observed (Fig. 2). Alternatively, such states may in fact be produced but are not observed because they are unreactive.

A more detailed examination of the relative threshold behavior of the three EI beams shows that as the electron energy is increased, the cross sections at the lowest reaction energies (< 1 eV) become enhanced. In addition, the peak at about 3 eV shifts slightly to lower energies. These observations confirm that the ratio of 5D to 5S increases with electron energy. We conclude that both states are present, reasonably reactive, and appear to form the same state of MnH^+ . Figure 3 shows a detailed comparison of the $Mn^+(SI)$ data with the $Mn^+(E_e = 25$ eV) data in the threshold region. The shapes of these curves are very similar up to 2.5 eV which suggests that the relative populations of the 5D and 5S states are also similar. Thus, while not obvious

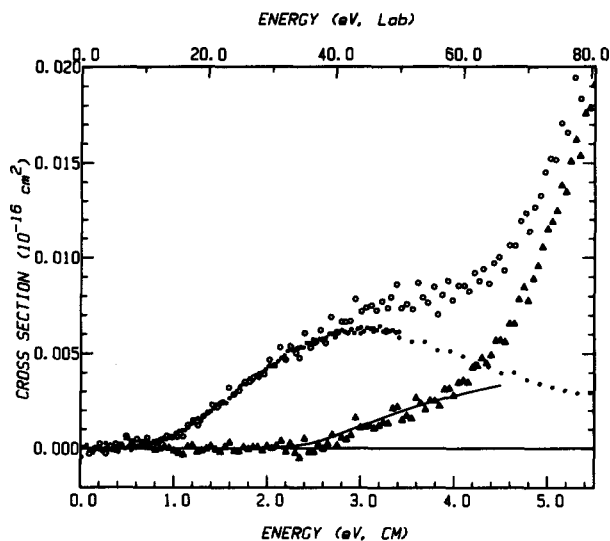


FIG. 3. Cross section in the threshold region for reaction of Mn⁺ with D₂ as a function of kinetic energy in the center-of-mass frame (lower scale) and laboratory frame (upper scale). Open circles (O) show the surface ionization (SI) data of Figs. 1 and 2 while closed circles (●) show the $E_e = 25$ eV data of Fig. 2 reduced by a factor of 21, Table III. Triangles (▲) are the difference between these two data sets. The line is a phase space calculation for reaction Mn⁺(⁷S) with D₂ convoluted with the experimental energy distribution and reduced by a factor of 909.

in Fig. 1, both the ⁵S(0.15% of the beam) and the ⁵D(0.03%) states of Mn⁺ are probably contributing in the reaction of Mn⁺(SI).

Threshold behavior

The state identifications made above can be made more definitive by further analysis of the threshold behavior of the low energy feature observed in Figs. 1–3. Based on the qualitative analysis above, we need to explicitly consider both the Mn⁺(⁵S) and Mn⁺(⁵D) states. In past work, the threshold behavior of reactions like process (1) has been modeled using simple empirical models.^{6,12} More recently, we have found that phase space theory (PST) provides a remarkably accurate description of the shapes of the threshold regions of many endothermic ion–molecule reactions (e.g., V⁺ + H₂)⁶ and in several cases (C⁺¹⁴, Si⁺¹⁵ + H₂; Al⁺ + O₂¹⁶), it can also predict the absolute magnitude of the cross sections within experimental error. Both empirical models and PST will be utilized here.

In the case of the empirical fitting procedure, the general form for the energy dependence of endothermic reaction cross sections is given by Eq. (6),

$$\sigma(E) = \sigma_0(E - E_T)^n/E^m. \quad (6)$$

Here, E is the relative kinetic energy, E_T is the reaction threshold, σ_0 is a scaling factor, and n and m are variable parameters. Comparison to the data is made after convoluting over the experimental energy distributions as described above. In our recent study of the reaction of V⁺ with hydrogen,⁶ we were able to show that in order to reproduce the data the values of E_T used in Eq. (6) has to be confined to a narrow range centered about the value obtained by a phase space theory analysis. In addition, the successful models in-

cluded the very simple line-of-centers (LOC) model given by $n = m = 1$. Similar results have been obtained for the reaction of Si⁺ with H₂ and D₂.¹⁷ Unfortunately, because the population of the excited states in the Mn⁺(SI) beam is extremely small, the quality of the data in the threshold region of Figs. 1 and 3 is insufficient for this type of comprehensive analysis. Consequently, in applying the empirical modeling approach to this system, we have confined ourselves to the LOC model. This is the most commonly used empirical model for interpreting reaction thresholds of metal ion–hydrogen reactions.¹²

The phase space calculations performed here use equations which are outlined elsewhere¹⁸ and molecular constants which are listed in Table II. Calculations include explicit consideration of all rotational states of H₂ (D₂) populated at 305 K, the temperature of the gas cell. Vibrational states are populated to a negligible degree. Comparison with the data is made after convoluting the theoretical cross sections with the experimental energy distributions. Two parameters are allowed to vary in the PST calculations, the reaction endothermicity (E_0) and the overall magnitude, until the data is best reproduced (as ascertained by a nonlinear least squares analysis). The threshold value, E_0 , obtained by this procedure differs slightly from E_T in that it is the threshold energy at 0 K.

For experiments where Mn⁺ is produced by surface ionization, five independent H₂ and four D₂ data sets were analyzed using both the LOC model and PST. The average values obtained for E_0 are 1.13 ± 0.06 eV for H₂ and 1.18 ± 0.09 eV for D₂. These two values should differ by the zero point energy difference in the reactions, 0.051 eV higher for the D₂ reaction.¹⁹ Thus, the average value for the endothermicity at 0 K for reaction with H₂ is 1.13 ± 0.07 eV. This reaction threshold energy can be related to the bond energy of MnH⁺ via Eq. (5) if we assume that there exists no barrier to reaction in excess of the endothermicity. If we explicitly include the possibility of electronic excitation, this yields Eq. (7),

$$D_0^{\circ}(\text{MnH}^+) = D_0^{\circ}(\text{H}_2) - E_0 - E_{el} \quad (7)$$

for the bond energy at 0 K. If we assume that both the ⁵S and ⁵D states have equal reactivity, the average electronic excitation of the Mn⁺(SI) beam is 1.27 ± 0.02 eV.²⁰ Using $D_0^{\circ}(\text{H}_2) = 4.477$ eV,¹³ this yields a bond energy of 2.08 ± 0.15 eV (47.9 ± 3.4 kcal/mol). The error is a conser-

TABLE II. Molecular constants (in cm⁻¹).

Species	B_e	ω_e	$\omega_e x_e^a$
MnH ⁺ ^b	5.9	1570	35.0
MnD ⁺ ^c	3.2	1120	17.4
H ₂ ^d	60.85	4401.2	121.34
D ₂ ^d	30.44	3115.5	61.82

^a Anharmonicity constant is calculated assuming a Morse oscillator potential well.

^b Reference 5.

^c Calculated from values for MnH⁺.

^d Reference 13.

vative two standard deviation estimate which includes the absolute uncertainty in the energy scale, 7 meV, see above.

Rather than use an average value for the electronic excitation in the Mn^+ (SI) beam, a better treatment would consider both the 5S and 5D states explicitly. While the scatter of the SI data makes such a treatment somewhat tenuous, this can be done if we assume that $E_0(^5S) - E_0(^5D) = 0.63$ eV, the difference in excitation energies, Table I. The result of such an analysis is $E_0(^5S) = 1.29$ eV for the D_2 reaction while the H_2 data contains too much scatter for a meaningful analysis. After zero point energy correction this value can be translated using Eq. (7) to $D_0^0(\text{MnH}^+) = 2.06$ eV (47.5 kcal/mol). This value, in good agreement with the bond energy derived above, is believed to be our best estimate of the true bond energy and is taken to have the same uncertainty, ± 0.15 eV.

Having ascertained the thermochemistry of reaction (1), we can now test two aspects of the phase space theory as applied to the Mn^+ system. First, the assumption that the 5S and 5D states have equal reactivity can be checked since the relative populations of these states need not be constrained. We find that the best fit to the data uses a relative population for $\text{Mn}^+(^5S)/\text{Mn}^+(^5D)$ of 6.7. This agrees closely with the calculated relative populations which range from 4.9 (at 2300 K) to 6.7 (at 2100 K), Table I. Second, we can compare the absolute magnitude of the PST calculation with the experimental data by multiplying the phase space cross sections by the experimental state populations, Table I. Interestingly, the absolute experimental cross section is also reproduced best when the excited state population is

TABLE III. Approximate populations of the Mn^+ beams.

Source ^a	State			Rel. ^c
	7S	$^5S^b$	$^5D^b$	
SI	1.0	0.0015	0.0003	1
25 eV	0.9	0.03	0.006	21
30 eV	0.7	0.05	0.017	40
50 eV	0.5	0.10	0.034	74

^a Source conditions for Mn^+ beams: SI, surface ionization at 2200 K, see Table I; other values refer to electron impact at the specified electron energy.

^b Errors are approximately $\pm 30\%$ for the 5S and $\pm 50\%$ for the 5D , see Table I.

^c Populations for the sum of the quintet states relative to that of the SI beam.

characteristic of a temperature of 2100 K. The result, shown in Fig. 4, is remarkably good considering the scatter in the data and the uncertainties in the beam temperature (changes in temperature of about 50 K lead to changes in the cross section of about 20%) and absolute cross sections ($\pm 20\%$). The final result of the preceding analysis demonstrates that the phase space calculation is able to predict the absolute magnitude of the excited state cross sections within the experimental uncertainty after adjusting the single parameter, E_0 .

Using the above results, we may examine the threshold region of the $E_e = 25, 30,$ and 50 eV excitation functions and determine the relative importance of the 5S and 5D states for these experiments. Using either the LOC model or PST, we are able to reproduce the data by adjusting the relative populations of the 5S and 5D states compared to the SI data. The results of this analysis, Table III, are not a direct measure of the state population but rather a function of relative population and reactivity. As noted above, however, the relative reactivity of these two states is apparently comparable. In all cases, the analysis finds that the 5S is the primary contribution to the low energy excitation function although the 5D does increase in importance with increasing electron energy. As noted above, the relative populations of the 5S and 5D states in the SI and $E_e = 25$ eV data appears comparable. This conclusion is verified by this analysis, Table III, and demonstrated nicely in Fig. 4. This shows that the same phase space analysis used to reproduce the SI data accurately reproduces the shape of the 25 eV data as well. The necessity of including the both 5S and 5D states is much more obvious in this comparison.

Table III also includes a rough estimate of the ground state populations in the Mn^+ beams produced by electron impact. This is obtained by comparison of the absolute cross sections at about 9 eV, Fig. 2. The fact that the sum of the 7S , 5S , and 5D state populations does not equal unity may indicate that higher lying excited states of Mn^+ are being populated. Based on the thermochemistry determined above, these states should react with hydrogen exothermically. As noted above, there is no evidence for such exothermic channels which implies that if present these excited states are unreactive. Alternatively, the discrepancy may be a reflex-

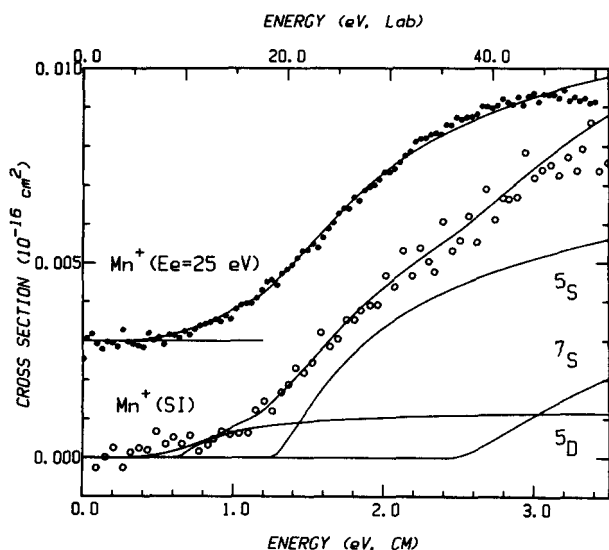


FIG. 4. Cross section in the threshold region for reaction of Mn^+ with D_2 as a function of kinetic energy in the center-of-mass frame (lower scale) and laboratory frame (upper scale). Open circles (\circ) show Mn^+ (SI) data while closed circles (\bullet) show $E_e = 25$ eV data reduced by a factor of 21, Table III, and offset from zero by 0.003 \AA^2 . Lines show the calculated phase space results for reaction of the 5S and 5D states of Mn^+ with populations characteristic of 2100 K and for reaction of the 7S state of Mn^+ divided by 909, see Fig. 3. The sum of these three curves convoluted with the experimental energy distribution is compared with the Mn^+ (SI) data. The sum of the 5S and 5D curves convoluted with the experimental energy distribution is compared with the Mn^+ ($E_e = 25$ eV) data.

tion of the rather large uncertainties in the determination of these populations.

Ground state cross section

The comparison between the Mn^+ (SI) and Mn^+ ($E_e = 25$ eV) data, Fig. 3, shows that the excited state cross sections decrease before the ground state cross section begins to rise rapidly at about 4.5 eV. The difference between these two curves is due solely to reaction of Mn^+ (7S) (although this assignment is not without uncertainty). This difference is shown in Fig. 3 and probably represents the true ground state cross section within an uncertainty of about 50%. Corroborating this identification is the observation that this excitation function has an apparent threshold which is quite close to the thermodynamic threshold for reaction of the 7S state with D_2 , 2.47 ± 0.15 eV. Using this value for the endothermicity, a phase space calculation of the Mn^+ (7S) reaction accurately predicts the shape of the cross section below 4 eV, Fig. 3. However, the absolute magnitude is ≈ 900 times smaller than the PST result. Since the 5S and 5D states appear to react with cross sections which are well described by PST, this factor can be taken as a measure of the relative reactivity of the ground and excited states.

$Mn^+ + HD$

Figure 5 contains the results for the reaction of Mn^+ (SI) with HD. Again, there are two features corresponding to the high and low energy features of the H_2 and D_2 reactions. The predominant high energy part begins at approximately 3 eV and peaks at 6 eV. Notice that the onset and peak occur earlier than those of the H_2 and D_2 reactions.

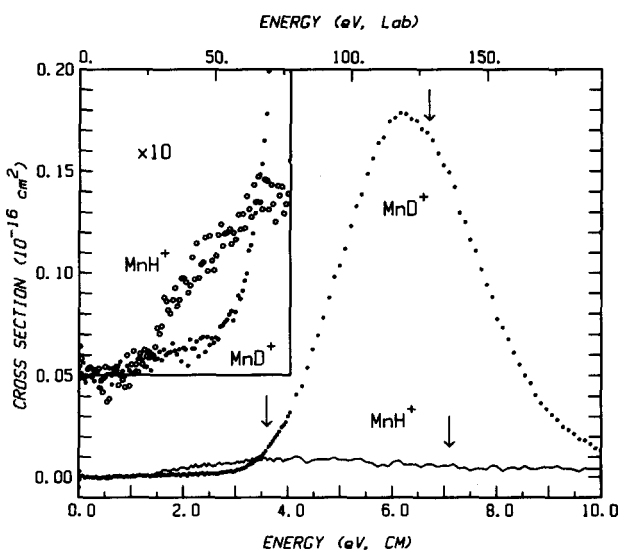


FIG. 5. Cross sections for reaction of Mn^+ (produced by surface ionization) with HD to form MnH^+ (line) and MnD^+ (points) as a function of kinetic energy in the center-of-mass frame (lower scale) and laboratory frame (upper scale). The inset shows the threshold data for MnH^+ (open circles) and MnD^+ (points) expanded by a factor of 10. Arrows indicate the pairwise threshold energy for production of MnD^+ at 3.6 eV, the pairwise dissociation energy of MnD^+ at 6.7 eV, and the pairwise threshold energy for production of MnH^+ at 7.1 eV, see the text and Table IV.

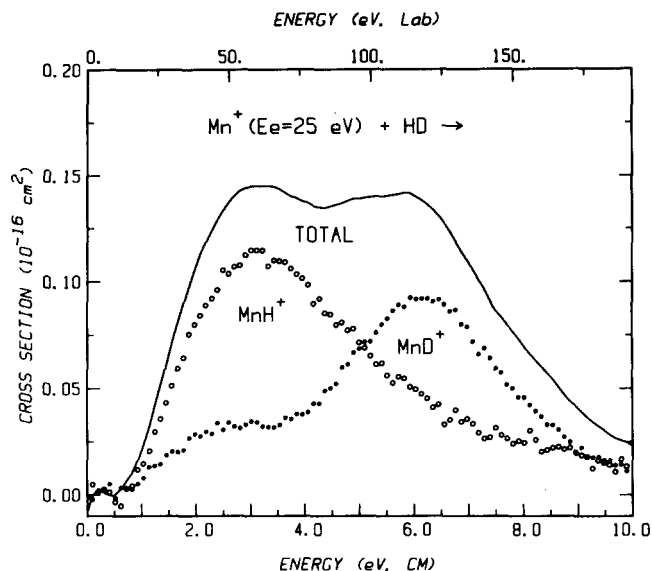


FIG. 6. Cross sections for reaction of Mn^+ (produced by electron impact at 25 eV) with HD to form MnH^+ (open circles) and MnD^+ (points) and their sum (line) as a function of kinetic energy in the center-of-mass frame (lower scale) and laboratory frame (upper scale).

The high energy feature produces MnD^+ almost exclusively. Such a large isotope effect is quite unusual and has not been reported previously for a transition metal ion reacting with HD. The low energy feature shows substantially different behavior. The reaction favors production of MnH^+ by about 3:1. The apparent threshold for both channels, ≈ 1 eV, is nearly the same as for the H_2 and D_2 reactions. A more comprehensive analysis of the thresholds of the low energy feature of the two product channels will not be performed due to scatter in the data.

Figures 6 and 7 show excitation functions for the reac-

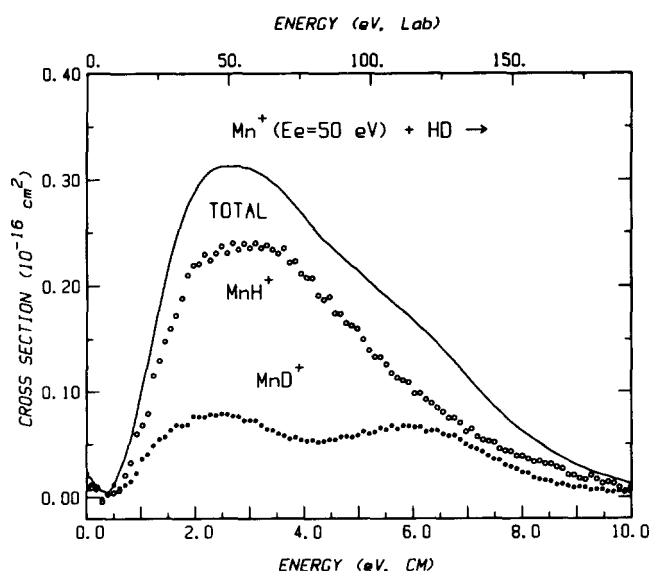


FIG. 7. Cross sections for reaction of Mn^+ (produced by electron impact at 50 eV) with HD to form MnH^+ (open circles) and MnD^+ (points) and their sum (line) as a function of kinetic energy in the center-of-mass frame (lower scale) and laboratory frame (upper scale).

tions of Mn^+ with HD where the ions have been produced by electron impact ionization ($E_e = 25$ and 50 eV, respectively). As for the D_2 data, the low energy feature (excited state reaction) grows while the high energy part (ground state reaction) diminishes with increasing electron energy. The fact that the isotope ratio for the low energy feature is 3:1 in favor of MnH^+ is now much more apparent. Modeling of this region seems to indicate that both the 5S and 5D states yield this approximate isotope ratio. The apparent threshold is again about 0.6 eV and the peak in the low energy feature is found at about 3 eV similar to the H_2 and D_2 results.

DISCUSSION

Thermochemistry

The bond energy for MnH^+ measured here, $D_0^{\circ}(MnH^+) = 2.06 \pm 0.15$ eV (47.5 ± 3.4 kcal/mol), is dependent on the proper identification of the states involved. The success of phase space theory in reproducing both the shape and absolute magnitude of the data lends confidence to the value derived. Our 0 K value differs from the 298 K literature values by $3/2kT = 0.039$ eV (0.9 kcal/mol). Our result for D_{298}° is 2.10 ± 0.15 eV (48.4 ± 3.4 kcal/mol). This value agrees, within the experimental uncertainties, with literature data, $D^{\circ} = 53 \pm 5$ kcal/mol,^{1,2} which also serves to substantiate our analysis. In fact, the agreement may be better than it first appears since the best literature value² is taken from a proton affinity (P.A.) measurement of Mn, $P.A.(Mn) = 195.5 \pm 2.5$ kcal/mol, relative to $P.A.(NH_3) = 207.0$ kcal/mol. This latter value is the subject of some controversy but values between 202 and 208 kcal/mol have been cited.^{21,22} If we choose $P.A.(NH_3) = 204 \pm 3$ kcal/mol,²² then $P.A.(Mn) = 192.5 \pm 4$ kcal/mol and the literature value for $D_0^{\circ}(MnH^+)$ becomes 49 ± 4 kcal/mol (2.13 ± 0.17 eV). The main point is that the value obtained in this study appears to be quite accurate.

This value is somewhat lower than recent citations of our work, 2.23 ± 0.1 eV.^{5,12(c)} This value did not include the complete state analysis performed above and hence is in error by approximately the average excitation due to the 5D state. The present value is also somewhat higher than results of *ab initio* calculations, $D_0^{\circ}(MnH^+) = 1.77$ eV (40.8 kcal/mol),³ 1.62 eV (37.4 kcal/mol),⁴ and 1.72 eV (39.6 kcal/mol),⁵ although it is closer than previous literature values. The *ab initio* results are expected⁵ to be systematically lower than experimental values by about 3 kcal/mol making the residual discrepancy about 5 kcal/mol. This is excellent agreement considering the extensive electron correlation which must be properly accounted for in the MnH^+ molecule. In fact, MnH^+ is probably the most difficult first-row transition metal hydride ion to calculate since the number of unpaired electrons is at a maximum.

Dynamics

In our recent study⁶ of the reactions of several electronic states of V^+ with H_2 , HD, and D_2 , we found that the relative reactivity of these states could be qualitatively understood using a simple molecular orbital (MO) diagram such as that shown in Fig. 8. The 5D ground state of V^+ which has a $3d^4$

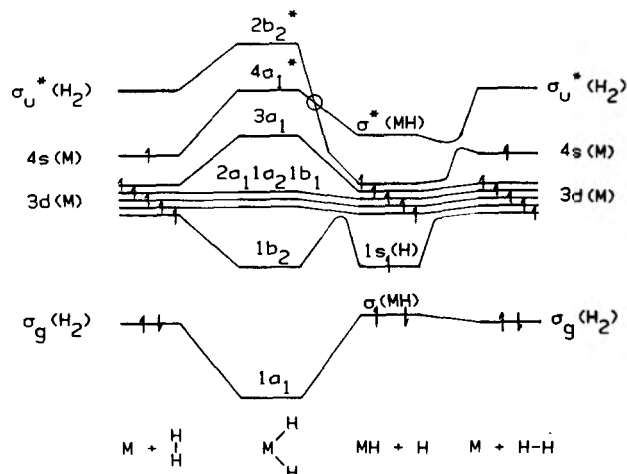


FIG. 8. Qualitative molecular orbital diagram for the interaction of a metal with H_2 in C_{2v} symmetry (left-hand side) and $C_{\infty v}$ symmetry (right-hand side). The electron populations shown are for ground state reactants, $Mn^+(^7S) + H_2(^1\Sigma_g^+)$, and for ground state products, $MnH^+(^6\Sigma) + H(^2S)$. The circle shows a crossing which becomes avoided in C_v symmetry.

electron configuration was found to react readily at threshold and yielded nearly equal amounts of VH^+ and VD^+ in the reaction with HD. This behavior was interpreted to indicate that this state inserts into the HD bond to form HVD^+ which then behaves statistically. For example, phase space theory predicts a $VH^+:VD^+$ ratio of about 0.7 . The 3F excited state of V^+ which has a $4s3d^3$ electron configuration shows comparable reactivity to the ground state but, in the reaction with HD, produces VH^+ with an abundance about $3-4$ times that of VD^+ . This isotope effect clearly indicates a much more direct reaction which we showed was consistent with angular momentum constraints in these heavy on light-light reaction systems.

This difference in behavior was rationalized using the MO diagram in Fig. 8. This shows that when the $4s$ or $3d\sigma$ orbitals on the metal ion are occupied, there is a strong repulsive interaction with the doubly occupied H_2 σ_g orbital (since an electron must be placed in the $3a_1$ or $4a_1$ orbital) when the reactants approach along a C_{2v} axis. In these situations, a $C_{\infty v}$ approach is preferred (similar to the $H + H_2$ reaction) and no long lived statistical intermediate can be formed. When the $4s$ and $3d\sigma$ orbitals are not occupied, insertion of the metal into the H_2 can occur readily to produce a metal dihydride intermediate (similar to $H^+ + H_2$).

The question we wish to address now is whether this simple analysis is useful for elucidating the relative reactivities of the Mn^+ states. First consider the excited states of Mn^+ , $^5S(4s3d^5)$ and $^5D(3d^6)$. We expect that both states should prefer a collinear reaction geometry since both must occupy the $3d\sigma$ orbital and the 5S state occupies the $4s$ as well. Experimentally, the reaction of both states proceeds efficiently at the thermodynamic limit and in the reaction with HD, production of MnH^+ is favored over MnD^+ by 3 to 1 . These observations are consistent with a collinear reaction geometry and are directly analogous to the results for $V^+(^3F,4s3d^3)$. Note too that the dynamics of $V^+(^5D,3d^4)$

differ from that of Mn⁺ (⁵D, 3d⁶). This difference is clearly explained using the MO diagram and is presumably a general result for comparing the reactivity of metal ions on the left-hand side of the periodic table with that of metal ions on the right-hand side.

Now consider the ground state reaction of Mn⁺. Like the ⁵S state, Mn⁺ (⁷S) has a 4s3d⁵ configuration. The MO diagram suggests that a C_{2v} approach would be strongly repulsive, as both 4s and 3dσ orbitals are occupied. We therefore expect a collinear configuration to be the lowest energy approach. In fact, *ab initio* calculations by Dupuis, Hammond, and Lester⁴ indicate that the preferred reaction geometry for this state is C_{∞v} and that there is no barrier in excess of the endothermicity for a trajectory with this symmetry. Despite the fact that the configurations of the ⁷S and ⁵S states are the same, the experimental results for their reaction differ appreciably. While there is a reaction pathway near the thermodynamic limit for Mn⁺ (⁷S) (see Fig. 3), it is very inefficient, ≈0.1%. The primary ⁷S reaction occurs at energies substantially in excess of the threshold and exhibits a very strong isotope effect unlike any reported for a transition metal ion reaction. These results are consistent with the MO model *only* if we presume that as the reaction geometry for Mn⁺ (⁷S) deviates from C_{∞v}, the potential energy rises rapidly. Since only a very small fraction of collisions are nearly collinear, reaction at threshold is inefficient. For off-collinear geometries, a second reaction mechanism, described in detail below, becomes effective at higher energies.

One possible explanation for this striking difference in reactivity between the ⁷S and ⁵S states of Mn⁺ could involve a spin restriction in going from reactants to products. However, MnH⁺ has a ⁶Σ(σ²3d⁵) ground state.⁵ Therefore, both spin and orbital angular momentum are conserved for reaction of either state of Mn⁺ with H₂(¹Σ) to form MnH⁺(⁶Σ) + H(²S). The true explanation must lie in a more detailed examination of the interactions of Mn⁺ with H₂. A convenient way to consider this is to look at the reaction in reverse, that is, at what happens when a H atom approaches MnH⁺(⁶Σ, σ²3d⁵). An exactly collinear approach of H to the hydride end of MnH⁺ would be overall attractive due to strong H–H bonding interactions. Because the *d* electrons on the manganese atom are largely core electrons and removed from the hydride end of the molecule, this attractive interaction should be similar regardless of the spin of the electron on the H atom. We therefore expect both a ⁷Σ and ⁵Σ surface which lead smoothly to Mn⁺ (⁷S) and Mn⁺ (⁵S), respectively, with little or no barrier. This is qualitatively the conclusions of *ab initio* calculations on the C_{∞v} approach,⁴ and is consistent with the experimental observations. As the reaction geometry departs from C_{∞v}, the incoming H atom begins to interact more extensively with the high spin *d* manifold of MnH⁺. If the H electron is aligned with the 3*d* electrons (high spin coupling, septet surface), an antibonding interaction occurs which is mediated by a favorable spin exchange interaction. Clearly, a node must exist between the incoming H(1*s*) electron and the 3*d* electrons. We expect an overall repulsive interaction which becomes severe as the geometry approaches C_{2v}. This is qualitatively the same conclusion drawn above by empirical considerations. If the H

electron approaches off the C_{∞v} axis such that it is low spin coupled with the 3*d* electrons of MnH⁺ (quintet surface), there can be a favorable bonding interaction but now mediated by a loss of exchange energy. Overall, a more favorable interaction is anticipated²³ and this is consistent with the high reactivity of the Mn⁺ (⁵S) state.

One final aspect of the potential energy surfaces which could influence the reactivity of the various electronic states involves surface crossings. It is possible that neither 4s3d⁵ state of Mn⁺ is able to react efficiently with H₂, perhaps due to their having occupied 4*s* and 3*d*σ orbitals, as discussed above. Reactions of 3*d*⁶ states, e.g., ⁵D, may be much more efficient since the 4*a*₁ orbital remains unoccupied, Fig. 8. Since there are no other septet states of Mn⁺, the ⁷S ground state cannot hop to another, more reactive surface. The ⁵S state, on the other hand, can interact with the ⁵D(3*d*⁶) state that is initially only 0.6 eV above it. An avoided crossing would mix these states and could allow Mn⁺ (⁵S) to react more efficiently than Mn⁺ (⁷S). Such a crossing also provides an explanation for how the ⁵S and ⁵D states could both lead to production of MnH⁺(⁶Σ). Since reaction of both states appears to be efficient, this *s*–*d* mixing seems to be fairly important. It will be of interest to have *ab initio* calculations, such as those recently performed on neutral systems,^{24,25} which can provide additional insight into these reasonably complex potential energy surfaces. It seems clear that such calculations need to consider off C_{2v} and off C_{∞v} reaction geometries.

Isotope effects for Mn⁺ (⁷S)

The final result deserving comment is the extraordinary isotope effect and energetics observed for the high energy reaction of Mn⁺ (⁷S). The most notable aspects of this process are: (1) the threshold shifts from ≈4.5 eV for the H₂ and D₂ reactions to ≈3.5 eV for formation of MnD⁺ from HD; (2) the peak of this reaction channel also shifts; and (3) little if any MnH⁺ is formed in reaction with HD. Qualitatively, this behavior can be understood in terms of a simple model which invokes impulsive pairwise interactions.²⁶ This means that the dominant mode of reaction depends primarily on the effective energy between the incoming ion and the atom with which it first interacts. For the general reaction,



the true center-of-mass energy is given by $E(\text{c.m.}) = \mu v^2/2$, where $\mu = A(B + C)/M$, $M = A + B + C$, the letters represent the masses of the atoms or molecular fragments in reaction (8), and v is the magnitude of the relative velocity of the reactants, $|\mathbf{v}(A) - \mathbf{v}(BC)|$. This is the energy scale on which Figs. 1–7 are plotted. If, however, the primary interaction is an impulsive collision between A and B, the effective energy is $E(\text{pair}) = \mu' v'^2/2$, where $\mu' = AB/(A + B)$ and v' is the same relative velocity since $\mathbf{v}(B) = \mathbf{v}(BC)$. The conversion between $E(\text{c.m.})$ and $E(\text{pair})$ is just

$$E(\text{pair}) = E(\text{c.m.}) \times MB/(A + B)(B + C) \quad (9)$$

such that the pairwise energy is always less than the true center-of-mass energy. Physically, a pairwise interaction always places a set fraction of the total available center-of-

TABLE IV. Pairwise interaction energies.

Reactant (BC)	H_2	HD^a	DH^a	D_2
Conversion factor ^b	0.51	0.35	0.68	0.52
Threshold energy (eV) ^c	4.7	7.1	3.6	4.7
Dissociation energy (eV) ^d	8.8	13.1	6.7	8.8

^a Boldface indicates the atom hit first, B, see the text.

^b This is given in Eq. (9). The mass of Mn = 54.9381 amu, H = 1.007 97 amu, and D = 2.014 amu.

^c $E(\text{c.m.})$ when $E(\text{pair}) = E_0(^7S)$, the thermodynamic threshold for reaction of $\text{Mn}^+(^7S)$ with BC to form MnB^+ , ≈ 2.4 eV.

^d $E(\text{c.m.})$ when $E(\text{pair}) = D^*(\text{BC}) \approx 4.5$ eV.

mass energy into relative translational motion of the three atoms. For reaction of Mn^+ with H_2 , HD, and D_2 , the fraction of energy left to cause reaction is given by the conversion factor of Eq. (9). These are listed in Table IV. Since $M \approx A \gg B, C$, these are nearly $B/(B+C)$ or $1/2$, $1/3$, $2/3$, and $1/2$ for reaction with H_2 , HD ($B = \text{H}$), DH ($B = \text{D}$), and D_2 , respectively. For the reaction with H_2 and D_2 , this leads to the expectation that on a center-of-mass scale reaction cannot occur until twice the thermodynamic threshold, $E_0(^7S) \approx 2.4$ eV, and that the MnH^+ product cannot begin decomposing [process (4)] until twice $D^*(\text{H}_2, \text{D}_2) \approx 4.5$ eV. Similarly, reaction with HD to form MnD^+ cannot occur until 1.5 times E_0 while formation of MnH^+ requires 3 times E_0 . Exact values of these predictions for all combinations of reactants are listed in Table IV. These values provide remarkably good agreement with the experimental onset of the high energy reaction feature and its peak for all three hydrogen isotopes, Figs. 1 and 5. It also suggests that reaction of $\text{Mn}^+(^7S)$ with HD should begin forming MnH^+ beginning about 7 eV. The failure to observe any such feature is somewhat puzzling but may be due to incomplete collection of this MnH^+ channel. This may not be the entire explanation, however, since the qualitative features expected from the pairwise interaction model have been observed in our laboratories for several other reactions of atomic ions with H_2 , HD, and D_2 .¹⁵ The fact that we do not observe the MnH^+ product from HD here but we do see the analogous product in other systems may imply that additional dynamical constraints are operating in the Mn^+ system.

One familiar model which incorporates the concept of pairwise interaction energies is the spectator stripping model (SSM).²⁷ Here, A hits B to form AB and no interaction with C (the spectator) takes place. The SSM is a highly specific example of a pairwise reaction which predicts that the cross section for reaction should begin at the threshold energy listed in Table IV and should go to zero at the dissociation energy listed in Table IV. The fact that the experimental data does not conform closely to the simple SSM means that the "spectator" atom *does* participate in the reaction. This participation places some of the available energy into relative product translation thereby stabilizing the diatomic product. This is, of course, quite reasonable especially considering that the reaction is endothermic, i.e., the reactant molecule has a stronger bond than the product molecule. The fact that

a pairwise energy scale is useful in describing the qualitative features of the reaction of $\text{Mn}^+(^7S)$ implies that the potential energy surface for approach of $\text{Mn}^+(^7S)$ to H_2 , HD, and D_2 is, at least for most geometries, quite repulsive. This is consistent with the discussion above.

CONCLUSION

The major results of the present study are as follows. One, the bond energy of MnH^+ has been measured as 2.06 ± 0.15 eV. This value is in good agreement with previously reported values and in reasonable agreement with recent *ab initio* calculations. Two, the $^7S(4s3d^5)$ state of Mn^+ reacts at its thermochemical threshold very inefficiently ($\approx 0.1\%$ of the phase space prediction). The major feature for reaction of this state occurs at energies well above this threshold. In the HD reaction, the major feature for reaction of $\text{Mn}^+(^7S)$ is also at unusually high energies, but shifted to lower energies than that for the H_2 or D_2 reaction. This feature exhibits an extraordinary isotope effect in which almost no MnH^+ is produced. The low reactivity at the thermochemical threshold is thought to be due to the existence of a barrier in the potential energy surface for off-collinear trajectories. The observed isotope effects and energy dependence for the high energy processes can then be explained in terms of an impulsive, pairwise collision model. Three, the $^5S(4s3d^5)$ and $^5D(3d^6)$ states of Mn^+ react efficiently at their thermochemical thresholds and produce ≈ 3 times as much MnH^+ as MnD^+ in the reaction with HD. This is believed to indicate that these reactions prefer to proceed via a collinear, direct process but that off-collinear trajectories are still reactive.

Four, the state dependence observed for the reactions of Mn^+ with H_2 and its isotopic analogs can be qualitatively understood using simple molecular orbital considerations. Similar considerations were also used to explain the results observed in a study of the reactions of several states of V^+ .⁶ Although these two reaction systems are dissimilar, taken together they probably represent the general trends for the left-hand and right-hand sides of the first row transition metal series. Specifically, metal ions with $3d^n$ configurations should react with H_2 via insertion when $n < 5$ [as $\text{V}^+(^5D)$] and by direct, collinear reaction when $n > 5$ [as $\text{Mn}^+(^5D)$]. Preliminary studies of other metal ions indicate behavior consistent with these expectations. For metal ions with $4s3d^n$ configurations, low spin coupled states are also anticipated to react via direct, collinear mechanisms [as seen for $\text{V}^+(^3F)$ and $\text{Mn}^+(^5S)$]. Reactions of states having high spin coupled $4s3d^n$ configurations (especially to the right-hand side) are expected to be inefficient [as for $\text{Mn}^+(^7S)$]. From preliminary work in this lab, it is apparent that the high spin $4s3d^n$ states of Cr^+ , Fe^+ , Co^+ , Ni^+ , and Cu^+ are relatively unreactive. It is less clear whether the high spin $4s3d^n$ states of Sc^+ , Ti^+ , and V^+ are also unreactive. Detailed studies of these metal ions are underway. It will be of interest to compare these results with the system described here as well as with the simple MO diagram predictions and other more sophisticated computational results as these become available.

ACKNOWLEDGMENTS

This work is supported by the National Science Foundation, Grant No. CHE-8306511. We would also like to thank the Monsanto Co.

- ¹(a) P. B. Armentrout, L. F. Halle, and J. L. Beauchamp, *J. Am. Chem. Soc.* **103**, 6501 (1981); (b) L. F. Halle, P. B. Armentrout, and J. L. Beauchamp, *Organometallics* **1**, 963 (1982).
- ²A. E. Stevens and J. L. Beauchamp, *Chem. Phys. Lett.* **78**, 291 (1981).
- ³M. A. Vincent, Y. Yoshioka, and H. F. Schaefer, *J. Phys. Chem.* **86**, 3905 (1982).
- ⁴M. Dupuis, B. L. Hammond, and W. A. Lester (private communication).
- ⁵J. B. Schilling, W. A. Goddard, and J. L. Beauchamp, *J. Am. Chem. Soc.* **108**, 582 (1986).
- ⁶J. L. Elkind and P. B. Armentrout, *J. Phys. Chem.* **89**, 5626 (1985).
- ⁷K. M. Ervin and P. B. Armentrout, *J. Chem. Phys.* **83**, 166 (1985).
- ⁸N. Aristov and P. B. Armentrout, *J. Am. Chem. Soc.* (in press).
- ⁹R. E. Winters and R. W. Kiser, *J. Phys. Chem.* **69**, 1618 (1965).
- ¹⁰R. H. Garstang, *Mon. Not. R. Astron. Soc.* **124**, 321 (1962); (private communication).
- ¹¹C. J. Lifshitz, R. L. C. Wu, T. O. Tiernan, and D. T. Terwilliger, *J. Chem. Phys.* **68**, 247 (1978).
- ¹²(a) P. B. Armentrout and J. L. Beauchamp, *Chem. Phys.* **50**, 37 (1980); *J. Am. Chem. Soc.* **103**, 784 (1981); (b) L. F. Halle, P. B. Armentrout, and J. L. Beauchamp, *ibid.* **103**, 962 (1981). (c) M. Mandich, L. F. Halle, and J. L. Beauchamp, *ibid.* **106**, 4403 (1984). (d) M. Tolbert and J. L. Beauchamp, *ibid.* **106**, 8117 (1984).
- ¹³K. P. Huber, G. Herzberg, *Molecular Spectra and Molecular Structure: Constants of Diatomic Molecules* (Van Nostrand Reinhold, New York, 1979).
- ¹⁴K. M. Ervin and P. B. Armentrout, *J. Chem. Phys.* (to be published).
- ¹⁵J. L. Elkind and P. B. Armentrout (work in progress).
- ¹⁶M. E. Weber, J. L. Elkind, and P. B. Armentrout, *J. Chem. Phys.* **84**, 1521 (1986).
- ¹⁷J. L. Elkind and P. B. Armentrout, *J. Phys. Chem.* **88**, 5454 (1984).
- ¹⁸W. J. Chesnavich and M. T. Bowers, *J. Chem. Phys.* **66**, 2306 (1977); D. A. Webb and W. J. Chesnavich, *J. Phys. Chem.* **87**, 3791 (1983).
- ¹⁹The zero point energy difference between H₂ and D₂ is 0.079 eV (Ref. 13). Using the vibrational constants given in Table II, the zero point energy difference between MnH⁺ and MnD⁺ is 0.028 eV. The zero point energy difference for reaction (1) is the difference between these values.
- ²⁰This is calculated from the relative populations, Table I, times the excitation energies summed over both states. Here, $0.85 \times 1.175 \text{ eV} + 0.15 \times 1.808 \text{ eV} = 1.27 \pm 0.02 \text{ eV}$.
- ²¹R. H. Staley, M. Taagepera, W. G. Henderson, I. Koppel, J. L. Beauchamp, and R. W. Taft, *J. Am. Chem. Soc.* **99**, 326 (1977); F. A. Houle and J. L. Beauchamp, *ibid.* **101**, 4067 (1979); S. T. Ceyer, P. W. Tiedemann, B. H. Mahan, and Y. T. Lee, *J. Chem. Phys.* **70**, 14 (1979).
- ²²S. G. Lias, J. F. Liebman, and R. D. Levin, *J. Phys. Chem. Ref. Data* **13**, 695 (1984).
- ²³It is interesting to note that calculations (Ref. 4) find a quasibound MnH₂⁺ (⁵B₂) species on the quintet surface. The fact that there is a substantial barrier to form this state (Ref. 4) presumably prevents this potential energy well from influencing the reaction dynamics observed here.
- ²⁴M. R. A. Blomberg and P. E. M. Siegbahn, *J. Chem. Phys.* **73**, 5682 (1983); P. E. M. Siegbahn, M. R. A. Blomberg, and C. W. Bauschlicher, *ibid.* **81**, 1373 (1984).
- ²⁵M. E. Ruiz, J. Garcia-Prieto, and O. Novaro, *J. Chem. Phys.* **80**, 1529 (1984); J. Garcia-Prieto, M. E. Ruiz, E. Poulain, G. A. Ozin, and O. Novaro, *ibid.* **81**, 5920 (1984); J. Garcia-Prieto, M. E. Ruiz, and O. Novaro, *J. Am. Chem. Soc.* **107**, 5635 (1985).
- ²⁶M. M. Chiang, B. H. Mahan, and C. Maltz, *J. Chem. Phys.* **57**, 5114 (1972); B. H. Mahan, *Interactions Between Ions and Molecules*, edited by P. Ausloos (Plenum, New York, 1975).
- ²⁷A. Henglein and K. Lacmann, *Adv. Mass Spectrom.* **3**, 331 (1966); A. Henglein, *Ion Molecule Reactions in the Gas Phase*, edited by P. J. Ausloos (American Chemical Society, Washington, D.C., 1966). A. Ding, K. Lacmann, and A. Henglein, *Ber. Bunsenges. Phys. Chem.* **71**, 596 (1967).